Death in the taste bud: Morphological features of dying taste cells and engulfment by Type I cells

Abbreviated Title: **Morphological features of dying murine taste cells**

Courtney E. Wilson, Robert S. Lasher, Ernesto Salcedo, Ruibiao Yang, Yannick Dzowo, John C. Kinnamon, Thomas E. Finger

Rocky Mountain Taste & Smell Center, University of Colorado School of Medicine, CU Anschutz Medical Campus, Aurora, CO 80045

Corresponding author: courtney.wilson@cuanschutz.edu

Number of pages: 37

Number of figures: 10

Number of tables: 1

Number of words:

Abstract: 236

Introduction: 646

Discussion: 1500

The authors declare no conflicts of interest.

This work was supported by National Institutes of Health National Institute on Deafness and Other Communication Disorders grants R01 DC017679, R01 DC014728, and R21 DC013186. The authors would like to acknowledge Dr. Graham Kidd and Emily Benson at the Lerner Research Institute at the Cleveland Clinic for their contribution to the data acquisition, which lead to this manuscript.

Abstract

Taste buds comprise 50-100 epithelial derived cells, which are renewed throughout the life of an organism. Immature cells enter the bud at its base, maturing into one of three distinct cell types. How taste cells die and/or exit the bud, however, remains unclear. Here we present morphological data obtained through Serial Blockface Scanning Electron Microscopy of murine circumvallate taste buds, revealing several taste cells at the end of their life (4-6 per bud). Cells we identify as dying share certain morphological features typical of apoptosis: swollen endoplasmic reticulum, large lysosomes, degrading organelles, distended outer nuclear membranes, heterochromatin reorganization, cell shrinkage, and cell and/or nuclear fragmentation. Based on these features, we divide the cells into “early” and “late” stage dying cells. Most early stage dying cells have Type II cell morphologies, while a few display Type III cell features. Many dying cells maintain contacts with nerve fibers, but those fibers often appear detached from the main trunk of an afferent nerve fiber. Dying cells, like mature Type II and Type III taste cells, are surrounded by Type I taste cells, the glial-like cells of the bud. In many instances Type I cells appear to be engulfing their dying neighbors, suggesting a novel, phagocytic role for Type I cells. Surprisingly, virtually no Type I cells, which have the shortest residence time in taste buds, display features of apoptosis. The ultimate fate of Type I cells therefore remains enigmatic.

Significance Statement

Our examination of serial EM sections through murine taste buds sheds light on the life cycle of taste cells—crucial components of our sense of taste. We find that dying taste cells exhibit features typical of programmed cell death, or apoptosis. Many dying cells retain contacts with nerve fibers, but those fibers are often disconnected from the nerve trunk, suggesting that they cannot signal to the brain. Interestingly, most dying cells are Type II cells, which detect bitter, sweet, or umami. Our data also suggest that glial-like Type I cells act as “undertakers” within taste buds, engulfing dying neighbors. Surprisingly, Type I cells, despite having the shortest lifespan, do not show signs of dying; their ultimate fate remains enigmatic.

Introduction

Taste buds comprise epithelial-derived cells, which are renewed repeatedly. Older cells die or leave the taste bud while newly post-mitotic immature cells enter from the base of the bud. To maintain accurate transmission of information to the central nervous system (CNS) in the face of wholesale receptor cell replacement, taste ganglion cells remodel their peripheral intragemmal arbors to disconnect from dying cells and reconnect to maturing taste cells (Whiddon et al., 2023).

We examined serial electron micrographs through taste buds to identify dying taste cells, predicting that the numbers and types of dying cells would be proportionate to both their relative abundance in the taste bud and the reported half-life for each population. Taste buds contain three types of mature taste cells, each unique in morphology, lifespan, and function. Type I cells, which constitute 60% of the mature cells in the bud (Yang et al., 2020), are considered glial-like (Murray et al., 1969; Pumplin et al., 1997), with an estimated lifespan of ~7 and ~16 days in rat and mouse, respectively (Farbman, 1980; Perea-Martinez et al., 2013). Type II cells, about one quarter of the cells in a bud, are spindle-shaped receptor cells and live for ~14-30 days (Perea-Martinez et al., 2013; Gross et al., 2017; Yang et al., 2020). Each responds to only one of the classical taste qualities: bitter, sweet, or umami, and perhaps amiloride-dependent sodium (Ohmoto et al., 2020). Type II cells communicate to nerve fibers via channel synapses, involving large-pore, voltage-gated channels associated with “atypical” mitochondria (Royer and Kinnamon, 1988; Chaudhari and Roper, 2010;

Taruno et al., 2013; Romanov et al., 2018). Type III cells are spindle-shaped cells, which constitute about 15-17% of the mature cells in a bud and are the most long-lived taste cells, with a half-life of at least 22 days (Perea-Martinez et al., 2013). Type III cells transduce ionic taste qualities, i.e. sour and highly salty stimuli, and communicate to nerves via vesicular synapses (Kinnamon et al., 1985; Yee et al., 2001; Huang et al., 2008; Yang et al., 2020).

To maintain structural architecture, taste buds must lose and gain cells at roughly the same rate. Organisms rid themselves of aging or unhealthy cells by three general mechanisms: apoptosis, autophagy, and necrosis (D'Arcy, 2019). Apoptosis is a form of programmed cell death resulting in characteristic ultrastructural changes: chromatin condensation, nuclear fragmentation, cell shrinkage, and ultimately the formation of apoptotic bodies that fragment off the cell. In contrast, in autophagy, which can either protect or kill a cell, macroproteins and organelles are sequestered into autophagosomes and are degraded. The process of necrosis results from acute injury to the cell; necrotic cells swell and rupture, spilling their contents and triggering an inflammatory response (D'Arcy, 2019; Chen et al., 2020). Only a few studies of cell death in the taste bud exist, and all report instances of apoptosis (Suzuki et al., 1996A; Takeda et al., 1996; Zeng and Oakley, 1999; Zeng et al., 2000; Huang and Lu, 2001; Ueda et al., 2008).

Here, using Serial Blockface Scanning Electron Microscopy (sbfSEM), we examine murine circumvallate taste cells for ultrastructural signs of cell death. This technique allows for the high-resolution imaging of serial sections through circumvallate taste tissue blocks (Yang et al., 2020; Wilson et al., 2022). In these buds, we find cells with ultrastructural features consistent with apoptosis. Given that Type I cells are the most abundant taste cell type and have the shortest half-life, we predicted that the majority of dying taste cells would be Type I cells. This was not the case; in fact, we observed no apoptotic Type I cells. Rather, apoptotic Type II and III cells are all at least partially surrounded by Type I taste cells, some quite substantially so. This arrangement and the presence of abundant, large lysosomes in Type I cells adjacent to dying cells suggests that Type I cells engulf and degrade dying cells within the taste bud.

Methods

Serial Block Face Scanning Electron Microscopy

As reported previously, Serial Blockface Scanning Electron Microscopy (sbfSEM) [see (Yang et al., 2020)] was used to generate two datasets from adult (>45 days) mouse circumvallate taste buds: DS2, composed of 563 sections, and TF21, composed of 633 sections. The data used in the present study were obtained primarily from two complete and one nearly complete taste buds from TF21 (Fig.1). A small number of cells from DS2 were also identified as early stage dying cells and more from this dataset were used for analysis of lysosomes. The original image data are freely available at the Electron

Microscopy Public Image Archive, part of the European Bioinformatics Institute (EMBL-EBI), in dataset EMPIAR-10331. Every taste cell in each section was assigned a unique identifier and was analyzed using Reconstruct software (Synapse Web Reconstruct, RRID:SCR_002716) (Fiala, 2005) to determine cell type and generate 3D reconstructions.

Identifying taste cells

Mammalian taste buds contain three basic types of mature taste cells: Type I, II, and III cells. We identified cells as being part of one of these categories based on several morphological features described in previous studies (Yang et al., 2020) (**Figure 1**). Type I cells tend to have elongate, invaginated nuclei, as well as thin, lamellar processes that extend around and between neighboring taste cells. While they often wrap around and border innervating nerve fibers, they do not display synaptic morphology (either atypical mitochondria or synaptic vesicles) at these sites of contact. The apical structure of Type I cells falls into two main categories: bushy, with many short microvilli, or arboriform, with one main microvillus with smaller microvillar “branches” (Yang et al., 2020). Type II cells are elongate, have a somewhat flattened fusiform shape, and relatively smooth, ovoid nuclei. The majority of Type II cells contain so called “atypical” mitochondria. These large mitochondria are characterized by tubular rather than stacked cristae and exist at points of synaptic contact from Type II cells onto afferent nerve fibers (Royer and Kinnamon 1988; Romanov et al., 2018) (**Figure 1B**). At their apical regions, Type II cells (e.g., **Figure 2A**) generally feature a single, large microvillus that extends far into the taste pore. Type III cells are elongate and spindle-shaped, with

a single, large microvillus that extends far into the taste pore and nuclei that are elongate and slightly invaginated (Yee et al., 2001; Yang et al., 2020). They are the only cells in the taste bud that form conventional, vesicular synapses onto afferent nerve fibers. These points of synaptic contact feature clear, 40-60nm diameter vesicles clustered at the plasma membrane region bordering the nerve fiber (**Figure 1C**).

Identifying lysosomes

The morphology of lysosomes can vary greatly over time and location in a cell (e.g., Dr. Jastrow's electron microscopic atlas, http://www.drjastrow.de/WAI/EM/EMAtlas.html.) Taste cell lysosomes appear to fall into two categories. The first category contains roughly spherical membrane-bound vesicles of about 150-600 nm in diameter containing packed, electron dense granules. The second category contains larger, irregularly shaped structures up to 1-2 microns in the longest dimension. These larger lysosomes have inclusions of electron dense material embedded in a matrix comprising a combination of somewhat electron dense material and electron lucent material. We segmented profiles of lysosomes in every section of selected cells, being careful not to include any tangential or cross-sections of mitochondria. Counts of lysosomes were performed using images taken from 3D reconstructions of cells primarily from dataset TF21.

Estimating ER distention

To estimate the size of dying cell endoplasmic reticulum regions as compared to those of healthy cells, we chose three healthy and three dying cells at random. In these cells, we randomly chose among sections containing the cell nucleus, using an online random number generator to select the section number, and used Photoshop (Adobe) to measure 5 separate sections of ER at their widest points from each cell. These values were then averaged for our estimates.

Nuclear Reconstructions and Display

Nuclear and taste bud perimeter traces were exported from the Reconstruct series files into MATLAB (Mathworks, Natick, MA) using custom MATLAB scripts (https://github.com/salcedoe/Dying_Taste_Cell_analysis). These traces were exported as a series of X, Y, and Z geometric vertices, which were organized in a table and sorted by cell identity and cell type. Vertices from individual nuclei were bound into 3D polyhedral meshes using the alphaShape function and visualized by plotting as 3D surface polygons.

Lysosome and Cell Volume Analysis

Cell and lysosomal traces were imported as geometric vertices into MATLAB as described for the nuclear reconstructions. The vertices were then grouped by cell identity and cell type. To determine lysosome size, vertices from lysosome traces were converted into Point Cloud objects using the pointCloud tool from the MATLAB Computer Vision Toolbox. These point clouds were then segmented into distinct lysosome clusters based on a set Euclidean distance using the MATLAB pcsegdist

function. Individual lysosome volumes were calculated by converting the lysosome point cloud clusters into 3D polyhedral meshes using the MATLAB alphaShape function, which then calculated the encased volume of each mesh. All generated 3D polyhedral surface meshes were visually inspected for morphological accuracy. Surface defects (e.g. large holes in the surface) were repaired using Manifold plus (https://github.com/hjwdzh/ManifoldPlus) and Meshfix 2.1 (https://github.com/MarcoAttene/MeshFix-V2.1). Taste cell volumes were then calculated from these inspected surface meshes. All cell meshes can be found on the github repository in the Lysosome Analysis/cellMeshes folder.

Statistical Analysis

MATLAB was used to calculate the statistics for the lysosome sizes. Comparisons between separate cell categories (i.e. healthy Type II cells, early stage dying Type II cells, healthy Type III cells, late stage dying cells, etc.) with regards to lysosome volumes were performed with Kruskal-Wallis and ANOVA tests, depending on whether datasets qualified as skewed by a Kolmogorov-Smirnov test. Comparisons between separate cell categories with regards to cell volumes were performed using estimation statistics on the median difference. (estimationstats.com ; Ho et al., 2019). The results of these cell volume estimation statistics are presented in **Supplemental Figure 1.**

Code/Software Accessibility

Code was generated for lysosome volume analysis and is readily available on GitHub (https://github.com/salcedoe/Dying_Taste_Cell_analysis).

Results

General features of dying taste cells and their nuclei

The taste cells that we identify as dying share several distinct morphological features that distinguish them from mature taste cells (**Figure 2**). In the cytoplasm of dying cells, abundant, swollen endoplasmic reticulum and large lysosomes are among the most readily apparent and common of these features. The endoplasmic reticulum of dying cells appears swollen in comparison to that of mature taste cells; the width (roughly perpendicular to the longitudinal axis) of ER segments in dying cells is ~250nm, while the same measurement in healthy cells is ~90nm (**Figure 2B, B', C, C'**). Healthy cells contain relatively small lysosomes, with median individual lysosome volumes ranging from 0.005-0.06 μm^3 per cell. In contrast, lysosomes in dying cells tend to be larger, with median lysosome volumes ranging from 0.004-0.12 μm^3 per cell (**Figure 2E, F, Figure 4**). Lysosome volumes differed significantly between the six different groups—I, II, III, IV, early dying, and late dying [Kruskal-Wallis test, $H(5, n=3904) = 328.2$, $p<0.0001$]. When we directly compared the lysosomes from healthy and early dying Type II cells in a post-hoc, multiple comparison analysis, we found the lysosomes in the dying cells to be significantly larger than the lysosomes in the healthy cells ($p<0.0001$). Mitochondria in dying cells often display signs of degradation—instead of the stacked cristae of healthy

mitochondria or the tubular cristae of atypical mitochondria, mitochondria in dying cells often contain irregular, sparse cristae (**Figure 2G**). Golgi bodies in dying cells, like the endoplasmic reticulum, appear swollen (**Figure 2I, I'**) when compared to those of healthy, mature taste cells (**Figure 2H, H'**). A subset of dying taste cells feature more obvious signs of apoptosis: cell shrinkage and even cell fragmentation into apoptotic bodies (**Figure 2A, D**). We deem these cells "late stage" dying cells, as opposed to the "early stage" dying cells, which are not fragmented and are still identifiable by cell type. Late stage dying cells are smaller than healthy cells, ranging in volume from 403-457 μm^3, while healthy Type II and III cells for which volume was measured range from 524-1172 μm^3. Interestingly, early stage dying Type II and III cells tend to be slightly larger than their healthy counterparts as well as late stage dying cells, ranging from 319-1984 μm^3 (**Figure 3, Supplementary Figure 1**). Late stage dying cells are fragmented into multiple separate objects. We presume these objects to be fragmented apoptotic bodies when they are in proximity to the main cell body and mirror its cytosolic qualities (**Figure 2D**).

Nuclei in dying cells likewise differ from those of mature taste cells (**Figure 5**). In dying cells that feature swollen endoplasmic reticulum and large lysosomes, the nuclear membranes exhibit clear, distended regions of separation between the inner and outer nuclear lamellae (**Figure 5B, C**). The degree of nuclear membrane separation varies among dying cells, with individual distended regions ranging from ~160 to 500 nm between the inner and outer leaflets (**Figure 5B, C, E', G'**). Since this intra-membrane

region is contiguous with the inner endoplasmic reticular space (Lindenboim et al., 2020), the distended nuclear membrane of dying cells may be an extension of the swollen endoplasmic reticulum, or vice versa. In a small subset of dying cells, nuclei feature accumulations of dense heterochromatin, a common characteristic of apoptotic cells (D'Arcy, 2019; Snigirevskaya and Komissarchik, 2019) (**Figure 5E', G'**). In one cell that appears to have fragmented into multiple apoptotic bodies, the nucleus is likewise fragmented into multiple bodies, which is consistent with caspase-induced breakdown of nuclear lamins (for review, Fink and Cookson, 2005) (**Figure 5E, E'**). Other nuclei in late stage dying cells possess large invaginations, which are perhaps harbingers to nuclear fragmentation (**Figure 5G, G'**).

Synapses in dying cells

The genesis and degeneration of taste cells necessitates remodeling of synaptic contacts and nerve fibers. To ascertain whether dying cells might still be communicating to taste nerves, we investigated possible synapses between dying cells and afferent nerve fibers. Late stage dying cells did not exhibit structures consistent with synapses onto afferent nerve fibers. At points of contact with nerve fibers, late stage dying cells lacked both the atypical mitochondria that characterize Type II cell synapses onto nerve fibers as well as the pre-synaptic clusters of vesicles that characterize Type III cell synapses onto nerve fibers (**Figure 6A**).

In contrast, most early stage dying cells were Type II cells still showed the presence of atypical mitochondria characteristic of synaptic contacts from this cell type. These atypical mitochondria appeared at sites of contact with nerve fibers, but these nerve fibers did not always exit the taste bud, suggesting nerve fiber fragmentation. This observation suggests that early stage dying Type II cells retain gross synaptic structures, but may not always be capable of signaling information to the CNS since the nerve fiber has fragmented (**Figure 6B, C**) and is no longer connected to the CNS. The atypical mitochondria in early stage dying Type II cells feature irregular, "loose" cristae (**Figure 6B**) when compared to the tubular cristae of atypical mitochondria in mature, healthy Type II cells (**Figure 1B**).

A minority of the early stage dying cells are Type III cells. These cells share similar cytoplasmic quality with early stage dying Type II cells, but lack atypical mitochondria. Instead, at points of contact with nerve fibers, we observe clear, membrane enclosed profiles that are larger than typical synaptic vesicles. Synaptic vesicles in healthy Type III cells range from 40-60 nm (Yang et al., 2020); membrane-bound objects at the site of contact between a dying Type III cell and a bordering nerve fiber range from ~30-300 nm. We tentatively mark these structures as degrading synaptic contacts, although the occurrence of signal transmission at these sites is unknowable with our current methods (**Figure 6D, E**). As with some fibers innervating early stage dying Type II cells, some nerve fibers contacting the putative early stage dying Type III cells do not exit the bud, suggesting nerve terminal fragmentation (**Figure 6F**). In TF21_ TB2, from which we have a complete connectome (Wilson et al., 2022), 4 of 7 (57%) nerve fibers innervating dying

cells are fragments that do not appear to exit the bud, while just 8 of 25 (32%) of nerve fibers innervating healthy cells appear to be fragments.

Type I cells engulf dying cells

Apoptotic cells elsewhere in the body are generally phagocytosed by elements of the immune system, often prior to the development of apoptotic bodies (D'Arcy, 2019). In the nasal epithelium, which is largely devoid of immune cells, sustentacular cells phagocytose neighboring epithelial cells (Suzuki et al., 1996B). Type I cells are considered the glial-like cells of the taste bud (for review, Chaudhari and Roper 2010). Type I cells possess diaphanous processes that extend around and between neighboring taste cells and are well positioned to engulf dying cells and any apoptotic bodies they might generate. Indeed, we observe signs of Type I cells engulfing dying cells and their fragmented apoptotic bodies (**Figure 7A-C**). In addition, membrane bound objects matching the cytosolic presentation of a dying cell are often seen in the cytoplasm of immediately adjacent Type I cells (**Figure 7C, E**). In regions of Type I cells that border dying cells, lysosomes tend to be larger, much like the lysosomes in the dying cells themselves (**Figure 4, Figure 7D, D''**). The 3 largest individual lysosomes in Type I cells range from 7.5-9.1 μm^3, which is several times the volume of the median volume lysosomes in either healthy or dying cells. In one case, a Type I cell that neighbors an early stage dying cell appears to have engulfed large, vacuous, membrane enclosed bodies. These bodies closely resemble the cytosolic appearance of the dying cell rather than the Type I cell itself. Thus, we presume this material originated in the dying cell

(**Figure 7E**). We have never observed either immune cells or other non-taste cells within the confines of the taste bud that could be involved in the elimination of dying cells.

Dying taste cells in the context of the bud

In total, we identify 21 dying cells in 5 different taste buds over two separate datasets. In the two taste buds wholly contained within the segmented block of tissue, 4 out of 84 and 5 out of 86 total taste cells appear to be dying according to our previously discussed morphological criteria. Of these dying cells, early stage dying cells are still identifiable as belonging to a mature taste cell type. These cells feature some, but not all, characteristics of dying cells. They tend to display swollen endoplasmic reticulum, degrading mitochondria, blebby nuclear membranes, swollen Golgi bodies, and large lysosomes. Of these early stage cells, most are Type II cells that maintain aspects of Type II cell morphology and atypical mitochondria. The remaining early stage dying cells share qualities with mature Type III cells. Late stage dying cells, however, could not be identified as to taste cell subtype, because of the more advanced signs of cell degradation: cell fragmentation, nuclear fragmentation, and notable reorganization of dense regions of heterochromatin in the nucleus. We thus label these cells as “unknown type” (**Figure 8A, Figure 9**).

Location of dying cells within the taste bud

Post-mitotic, immature Type IV taste cells are known to enter the taste bud near the basilar membrane and inhabit the bottom 1/3 of the bud (Barlow, 2015; Yang et al.,

2020). As they mature, taste cells extend into the upper portions of the bud, eventually reaching the taste pore. We hypothesized that dying cells would be restricted to the upper regions of the taste bud, farther away from their origins in the basal regions of the bud. Indeed, the nuclei of dying cells tend to be in the top 1/3 of the taste bud, although taste cells at the upper extremities of the bud do not all display hallmarks of degeneration (**Figure 8B**).

Discussion

The data we present suggest an apoptotic pathway for the death of Type II and III taste receptor cells (**Figure 9**). As the cells progress towards death, the ER and Golgi swell, lysosomes enlarge, mitochondrial cristae become disorganized, and the inner and outer leaflets of the nuclear membrane separate (**Figures 2, 4, and 5**). These features are consistent with apoptosis (D'Arcy, 2019; Snigirevskaya and Komissarchik, 2019), and agree with reports of apoptotic markers within taste buds (Zeng and Oakley, 1999; Zeng et al., 2000; Huang and Lu, 2001; Takeda et al., 1996). Early stage dying cells tend to be larger than healthy or late stage cells, indicating that cells swell slightly before late stage cell death (**Figure 3**). As cells progress to the late dying stage, heterochromatin reorganization becomes more pronounced, cell volume reduces, and apoptotic bodies separate from the main cell body (**Figures 2, 3, and 5**).

We conclude that the dying cells we describe are undergoing apoptosis. If taste cells were dying by non-apoptotic methods, we would expect different morphologies. Cells undergoing necrosis manifest substantial cell swelling, extracellular spillage of cell contents, and infiltration of immune cells (D'Arcy, 2019; Lakshmanan et al., 2022). Instead, we observe cell shrinkage in late stage dying cells, formation of putative apoptotic bodies, and no evidence of immune cell infiltration. Interestingly, early stage dying cells are slightly larger than healthy cells (**Figure 3, Supplementary Figure 1**). That cells swell before shrinking is not necessarily inconsistent with apoptosis. Reduced ATP production on account of degrading mitochondria might disrupt the Na^+/K^+-ATPase, which can result in swelling (Chen et al., 2014). In autophagy, dying cells would form autophagosomes, which sequester and degrade macroproteins and organelles (Eskelinen et al., 2011). We do not observe such structures in dying Type II or III cells, although autophagosome-like structures occasionally appear in Type I cells. However, we cannot determine if these structures indicate cell death or repair.

In the two complete buds contained within the samples, few cells per bud appear to be undergoing apoptosis: 4 of 84 (4.7%) and 5 of 86 (5.8%). Some previous studies estimate the dying cell population at 1-3 dying cells per bud (Ueda et al., 2008; Huang and Lu, 2001; Takeda et al., 1996), while others estimate it at ~9 cells per bud (Zeng and Oakley, 1999; Zeng et al., 2000) (**Table 1**). Our observed prevalence of apoptotic cells may be higher than the lower estimates due to the relatively short period (1-3 hrs) during which an apoptotic cell is positive for classical apoptotic markers, i.e. TUNEL and ssDNA

(Gavrieli et al., 1992). The studies that estimated a larger dying cohort used p53 and Caspase-2 as markers, both of which are initiating apoptotic factors whose presence likely precedes the morphological changes we report (Zeng and Oakley 1999; Zeng et al., 2000, Bouchier-Hayes and Green, 2012). Beidler and Smallman (1965) reported that rat taste buds lose approximately half their cells every 10 days. If mouse taste buds are similar, we expect 4-5 dying cells per day in a bud of 80-100 cells. Our results are consistent with this estimate.

Of early stage dying taste cells, the majority are Type II cells and a few are Type III cells. Buds contain fewer Type III than Type II cells, and Type III cells are the longest-lived, making it less likely that we would observe them dying in a single snapshot of a dynamic organ. Surprisingly, we do not observe apoptotic Type I cells. Type I cells are the most common (~50% of all cells; Yang et al., 2020), and are described as the shortest-lived (Farbman, 1980; Perea-Martinez et al., 2013; Gross et al., 2017; Yang et al., 2020). If a bud contains ~100 cells, we expect ~50 to be Type I cells. If, as according to the estimates of Beidler and Smallman (1965) and Yang et al (2020), half of this population is renewed every 10 days, then we would expect ~2.5 Type I cells dying per day in each taste bud. Since this estimate is based on the entire taste cell population, and Type I cells reportedly have the shortest lifespan (Farbman, 1980; Hamamichi et al., 2006; Perea-Martinez et al., 2013; Gross et al., 2017), the estimate is likely conservative. However, we do not observe apoptotic Type I cells. What then, is their ultimate fate? Ueda and colleagues reported a population of apoptotic cells interpreted as Type I cells

in rats (Ueda et al., 2008). The marker used to identify these cells (human blood antigen H) is, however, not specific to Type I cells (Ueda et al., 2003). Other estimates of Type I cell lifespans are based on perdurance of nucleotide labeling during progenitor cell division; Farbman (1980) estimated “dark” cells (an earlier term apparently equivalent to Type I cells) to have a lifespan of ~7 days, and Perea-Martinez (2013) and colleagues found cells lacking Type II or III markers (presumed Type I cells) to have a ~16 day lifespan. If Type I cells are exiting the bud rather than dying, previous studies would not necessarily capture that process. Conceivably, Type I cells may exit the taste bud apically or laterally, to be eventually sloughed off the lingual epithelium with non-taste epithelial cells. Alternatively, Type I cells may be dying too quickly to capture in our sampling paradigm, or may die via an alternative cell death process which shows no obvious morphological features. We do occasionally observe autophagosome-like profiles in Type I cells, but cannot determine whether these structures indicate cell death, cell repair, or phagocytosis of neighboring dying cells. Possibly, the Type I cells undergo autophagy following phagocytosis of other dying cells. The cells we describe as late stage dying cells could include Type I cells, but are more rare than expected. Our data do not resolve how and whether Type I cells die or otherwise exit the taste bud.

Early stage dying Type II and III cells feature synaptic structures in various stages of degradation, suggesting impaired signaling to nerves. Moreover, these dying cells often contact postsynaptic nerve fibers that, seemingly, do not exit the bud and thus cannot signal to the CNS. In the face of wholesale turnover of taste receptor cells, taste nerves

426 are constantly remodeling (Whiddon et al., 2023). Large “end-bulbs” are associated with
427 nerve branch retraction (Zaidi et al., 2016; Whiddon et al., 2023) and we occasionally
428 observe enlarged nerve processes near late stage dying cells (**Figure 6A**). More often,
429 synapses from dying cells contact nerve fiber fragments (**Figure 6B-F**). Considering these
430 data, we hypothesize that nerve fiber fragments that receive synapses from early stage
431 dying cells have separated from their trunk nerve fibers as a part of the remodeling
432 process. Such nerve fragments are not reported by Whiddon et al (2023), who rely on
433 sparse GFP label to follow individual fibers within a taste bud. A possible explanation for
434 this discrepancy is that once a nerve fiber fragment detaches from the nerve trunk, it’s
435 ability to maintain pH homeostasis degrades, which would cause cytoplasmic
436 acidification and could quench the GFP fluorescence (Roberts et al., 2016). We cannot,
437 however, rule out the possibility that these nerve fiber fragments are attached to fibers
438 exiting the bud, but that our data do not allow us to accurately trace the full nerve
439 profile. In our dataset, it can be challenging to follow processes with diameters less than
440 70 nm (the section thickness) as they wend their way between other cell and fiber
441 processes.
442
443 Our data present a novel role for Type I cells in the taste bud, i.e. Type I cells engulf and
444 remove neighboring apoptotic cells. In many tissues, immune cells fill this phagocytic
445 role (D’Arcy, 2019) but we find no evidence for immune cells within taste buds. Type I
446 cells, considered the glial-like support cells of the taste bud, are well poised for a
447 phagocytic role. Precedence exists for supporting cells in sensory epithelia engulfing

448 dying cells, as in the olfactory epithelium (Suzuki et al., 1996B). Previous studies found
449 Type I taste cells containing large, dense bodies within their cytosol (Takeda et al., 1996;
450 Farbman, 1969; Fujimoto and Murray 1970; Olivieri-Sangiacomo, 1970; Farbman, 1985).
451 Our data are consistent with these observations, leading us to the hypothesis that Type I
452 cells phagocytose and degrade materials from apoptotic Type II and III cells.
453
454 These data point to apoptosis as a major mechanism of death for murine taste cells. The
455 dying cells we identify feature several hallmarks of apoptosis, and can be categorized
456 into either early or late stages of death. Those that retain synaptic contacts with nerve
457 fibers during early stages of cell death are likely impaired in their ability to communicate
458 to the CNS, as many of their target nerve fibers are fragmented. Type I cells appear to
459 engulf dying cells, identifying a novel, phagocytic role for Type I taste cells. We do not,
460 however, identify morphologically recognizable Type I cells in the process of cell death.
461 Whether, how, and when Type I cells die or exit the taste bud remains unclear.
462

463 **References**

464 Barlow LA (2015). Progress and renewal in gustation: new insights into taste bud development.
465 *Development*, *142*(21), 3620-3629.

466

467 Beidler LM, Smallman RL (1965). Renewal of cells within taste buds. J Cell Biol, 27(2),
468 263-272.

469

470 Bouchier-Hayes, L., & Green, D. R. (2012). Caspase-2: The orphan caspase. *Cell Death Differ*,
471 *19*(1), 51-57.

472

473 Chaudhari N, & Roper SD (2010). The cell biology of taste. J Cell Biol, 190(3), 285-296.

474

475 Chen D, Song M, Mohamad O, Yu SP (2014). Inhibition of Na+/K+-ATPase induces hybrid
476 cell death and enhanced sensitivity to chemotherapy in human glioblastoma cells. BMC
477 Cancer, 14, 716.

478

479 Chen Y, Hua Y, Li X, Arslan IM, Zhang, W., & Meng, G. (2020). Distinct Types of Cell Death
480 and the Implication in Diabetic Cardiomyopathy. Front Pharmacol, 11, 42.

481

482 Clapp TR, Medler KF, Damak S, Margolskee RF, Kinnamon SC (2006). Mouse taste cells
483 with G protein-coupled taste receptors lack voltage-gated calcium channels and SNAP-
484 25. BMC Biol, 4, 7.

D'Arcy MS (2019). Cell death: a review of the major forms of apoptosis, necrosis and autophagy. Cell Biol Int, 43(6), 582-592.

Eskelinen EL, Reggiori F, Baba M, Kovacs AL, Seglen PO (2011). Seeing is believing: the impact of electron microscopy on autophagy research. Autophagy, 7(9), 935-956.

Farbman AI (1969). Fine structure of degenerating taste buds after denervation. Journal of Embryology and Experimental Morphology, 22(1), 55-68.

Farbman AI (1980). Renewal of taste bud cells in rat circumvallate papillae. Cell Tissue Kinet, 13(4), 349-357.

Farbman AI, Hellekant G, Nelson A (1985). Structure of taste buds in foliate papillae of the rhesus monkey, Macaca mulatta. Am J Anat, 172(1), 41-56.

Fiala JC (2005). Reconstruct: a free editor for serial section microscopy. J Microsc, 218(Pt 1), 52-61.

Fink SL, Cookson BT (2005). Apoptosis, pyroptosis, and necrosis: mechanistic description of dead and dying eukaryotic cells. Infect Immun, 73(4), 1907-1916.

507 Fujimoto S, Murray RG (1970). Fine structure of degeneration and regeneration in
508 denervated rabbit vallate taste buds. Anat Rec, 168(3), 383-413.
509
510 Gavrieli Y, Sherman Y, Ben-Sasson SA (1992). Identification of programmed cell death in
511 situ via specific labeling of nuclear DNA fragmentation. J Cell Biol, 119(3), 493-501.
512
513 Gross L, Scott JK, Castillo Azofeifa D, Gaillard D, Barlow LA (2017). Molecular genetic
514 lineage tracing of taste bud cells in adult mice. AChemS, Bonita Springs, FL.
515
516 Hamamichi R, Asano-Miyoshi M, Emori Y (2006). Taste bud contains both short-lived and
517 long-lived cell populations. Neuroscience, 141(4), 2129-2138.
518
519 Ho J, Tumkaya T, Aryal S, Choi H, Claridge-Chang A (2019). Moving beyond P values: data
520 analysis with estimation graphics. Nat Methods, 16(7), 565-566.
521
522 Huang YA, Maruyama Y, Stimac R, Roper SD (2008). Presynaptic (Type III) cells in mouse
523 taste buds sense sour (acid) taste. J Physiol, 586(12), 2903-2912.
524
525 Huang YJ, Lu KS (2001). TUNEL staining and electron microscopy studies of apoptotic
526 changes in the guinea pig vallate taste cells after unilateral glossopharyngeal
527 denervation. Anat Embryol (Berl), 204(6), 493-501.
528

529 Kinnamon JC, Taylor BJ, Delay RJ, Roper SD (1985). Ultrastructure of mouse vallate taste
530 buds. I. Taste cells and their associated synapses. J Comp Neurol, 235(1), 48-60.
531
532 Lakshmanan HG, Miller E, White-Canale A, McCluskey LP (2022). Immune responses in
533 the injured olfactory and gustatory systems: a role in olfactory receptor neuron and
534 taste bud regeneration? Chem Senses, 47.
535
536 Lindenboim L, Zohar H, Worman HJ, Stein R (2020). The nuclear envelope: target and
537 mediator of the apoptotic process. Cell Death Discov, 6, 29.
538
539 Medler KF, Margolskee RF, Kinnamon SC (2003). Electrophysiological characterization of
540 voltage-gated currents in defined taste cell types of mice. J Neurosci, 23(7), 2608-2617.
541
542 Murray RG, Murray A, Fujimoto S (1969). Fine structure of gustatory cells in rabbit taste
543 buds. J Ultrastruct Res, 27(5), 444-461.
544
545 Ohman LC, Krimm RF (2021). Whole-Mount Staining, Visualization, and Analysis of
546 Fungiform, Circumvallate, and Palate Taste Buds. J Vis Exp(168).
547
548 Ohman LC, Krimm RF (2021). Variation in taste ganglion neuron morphology: insights
549 into taste function and plasticity. Curr Opin Physiol, 20, 134-139.
550

551 Ohmoto M, Jyotaki M, Foskett JK, Matsumoto I (2020). Sodium-Taste Cells Require Skn-
552 1a for Generation and Share Molecular Features with Sweet, Umami, and Bitter Taste
553 Cells. eNeuro, 7(6).
554
555 Olivieri-Sangiacomo C (1970). Ultrastructural modifications of denervated taste buds. Z
556 Zellforsch Mikrosk Anat, 108(3), 397-414.
557
558 Perea-Martinez I, Nagai T, Chaudhari N (2013). Functional cell types in taste buds have
559 distinct longevities. PLoS One, 8(1), e53399.
560
561 Pumplin DW, Yu C, Smith DV (1997). Light and dark cells of rat vallate taste buds are
562 morphologically distinct cell types. J Comp Neurol, 378(3), 389-410.
563
564 Roberts TM, Rudolf F, Meyer A, Pellaux R, Whitehead E, Panke S, Held M (2016).
565 Identification and Characterisation of a pH-stable GFP. Sci Rep, 6, 28166.
566
567 Rodriguez YA, Roebber JK, Dvoryanchikov G, Makhoul V, Roper SD, Chaudhari N (2021).
568 "Tripartite Synapses" in Taste Buds: A Role for Type I Glial-like Taste Cells. J Neurosci,
569 41(48), 9860-9871.
570
571 Romanov RA, Lasher RS, High B, Savidge LE, Lawson A, Rogachevskaja OA, Zhao H,
572 Rogachevsky VV, Bystrova MF, Churbanov GD, Adameyko I, Harkany T, Yang R, Kidd GJ,

573 Marambaud P, Kinnamon JC, Kolesnikov SS, Finger TE (2018). Chemical synapses without
574 synaptic vesicles: Purinergic neurotransmission through a CALHM1 channel-
575 mitochondrial signaling complex. Sci Signal, 11(529).
576
577 Roper SD (2013). Taste buds as peripheral chemosensory processors. Semin Cell Dev
578 Biol, 24(1), 71-79.
579
580 Royer SM, Kinnamon JC (1988). Ultrastructure of mouse foliate taste buds: synaptic and
581 nonsynaptic interactions between taste cells and nerve fibers. J Comp Neurol, 270(1),
582 11-24, 58-19.
583
584 Snigirevskaya ES, Komissarchik YY (2019). Ultrastructural traits of apoptosis. Cell Biol Int,
585 43(7), 728-738.
586
587 Suzuki Y, Takeda M, Farbman AI (1996). Supporting cells as phagocytes in the olfactory
588 epithelium after bulbectomy. J Comp Neurol, 376(4), 509-517.
589
590 Suzuki Y, Takeda M, Obara N, Nagai Y (1996). Phagocytic cells in the taste buds of rat
591 circumvallate papillae after denervation. Chem Senses, 21(4), 467-476.
592
593 Takeda M, Suzuki Y, Obara N, Nagai Y (1996). Apoptosis in mouse taste buds after
594 denervation. Cell Tissue Res, 286(1), 55-62.

Taruno A, Vingtdeux V, Ohmoto M, Ma Z, Dvoryanchikov G, Li A, Adrien L, Zhao H, Leung S, Abernethy M, Koppel J, Davies P, Civan MM, Chaudhari N, Matsumoto I, Hellekant G, Tordoff MG, Marambaud P, Foskett JK (2013). CALHM1 ion channel mediates purinergic neurotransmission of sweet, bitter and umami tastes. Nature, 495(7440), 223-226.

Ueda K, Fujii M, El-Sharaby A, Honma S, Wakisaka S (2003). Human blood group antigen H is not the specific marker for type I cells in the taste buds. Arch Histol Cytol, 66(5), 469-473.

Ueda K, Ichimori Y, Maruyama H, Murakami Y, Fujii M, Honma S, Wakisaka S (2008). Cell-type specific occurrence of apoptosis in taste buds of the rat circumvallate papilla. Arch Histol Cytol, 71(1), 59-67.

Whiddon ZD, Marshall JB, Alston DC, McGee AW, Krimm RF (2023). Rapid structural remodeling of peripheral taste neurons is independent of taste cell turnover. PLoS Biol, 21(8), e3002271.

Wilson CE, Lasher RS, Yang R, Dzowo Y, Kinnamon JC, Finger TE (2022). Taste Bud Connectome: Implications for Taste Information Processing. J Neurosci, 42(5), 804-816.

Yang R, Crowley HH, Rock ME, Kinnamon JC (2000). Taste cells with synapses in rat circumvallate papillae display SNAP-25-like immunoreactivity. J Comp Neurol, 424(2), 205-215.

Yang R, Dzowo YK, Wilson CE, Russell RL, Kidd GJ, Salcedo E, Lasher RS, Kinnamon JC, Finger TE (2020). Three-dimensional reconstructions of mouse circumvallate taste buds using serial blockface scanning electron microscopy: I. Cell types and the apical region of the taste bud. J Comp Neurol, 528(5), 756-771.

Yee CL, Yang R, Bottger B, Finger TE, Kinnamon JC (2001). "Type III" cells of rat taste buds: immunohistochemical and ultrastructural studies of neuron-specific enolase, protein gene product 9.5, and serotonin. J Comp Neurol, 440(1), 97-108.

Zaidi FN, Whitehead MC (2006). Discrete innervation of murine taste buds by peripheral taste neurons. J Neurosci, 26(32), 8243-8253.

Zeng Q, Oakley B (1999). p53 and Bax: putative death factors in taste cell turnover. J Comp Neurol, 413(1), 168-180.

Zeng, Q., Kwan, A., & Oakley, B. (2000). Gustatory innervation and bax-dependent caspase-2: participants in the life and death pathways of mouse taste receptor cells. *J Comp Neurol*, *424*(4), 640-650.

638 Table 1. Reported numbers of dying cells in taste buds.

Citation	Animal model	Death identification method	Observed dying cells per section	If bud = 40 µm across, dying cells/bud
Ueda et al 2008	Rat	ssDNA stain	1.2 cells / 16 µm section	~3
Zeng & Oakley 1999	Mouse	p53 (early death signal)	11.4%	11.4% (~9 cells)
Zeng et al 2000	Mouse	Caspase-2 (protease)	11% +/- 0.8%	11% (~9 cells)
Huang & Lu 2001	Guinea pig	Tunel stain	~1-2 tunel+ cells / 20 µm section	2-4
Takeda et al 1996	Mouse	Tunel stain	~0.14 tunel+ cells / 6 µm section	0.93

639

640

Figure 1. Taste cell types and synapses in murine circumvallate taste buds. A. Electron micrograph of a circumvallate mouse taste bud with overlaid individual reconstructions of a Type I cell (green), Type II cell (blue), Type III cell (red), and Type IV immature cell (purple). Scale bar is 10 µm. **B.** Micrograph of the channel synapse between a Type II cell (blue) and adjacent nerve fiber (yellow) with arrows indicating the large, atypical mitochondria characteristic of Type II cell synapses. Scale bar is 1 µm for both **B** and **C**. **C.** Micrograph of the synapse between a Type III cell (red) and adjacent nerve fiber (yellow) with arrow indicating the cluster of vesicles at the pre-synaptic membrane.

Figure 2. Morphological features of healthy and dying taste cells. A. Reconstruction of a healthy, mature Type II cell (blue) in the taste bud shell (gray). Scale bar is 10 µm. **B.** Micrograph of a healthy Type II cell, with arrows indicating endoplasmic reticulum (ER). Scale bar is 2 µm and applies to **B, C, E,** and **F**. **B'**. Enlarged region of healthy Type II cytosol showing normal ER (arrows). Scale bar is 1 µm. **C.** Micrograph of a dying Type II cell, with arrows indicating examples of swollen endoplasmic reticulum. **C'.** Enlarged region of dying Type II cell cytosol, featuring swollen endoplasmic reticulum. Scale bar is 1 µm. **D.** Reconstruction of a dying cell of unknown type (purple) in the taste bud shell (gray). Scale is the same as in **A**. **D'.** Enlarged region of dying taste cell reconstruction in **D**. Arrow indicates the point of separation between the main dying cell and its apical fragment. **E.** Micrograph of healthy Type II cell, with an arrow indicating the only visible lysosome in this cell profile. **F.** Micrograph of a dying Type II cell, with arrows indicating some of the numerous lysosomes apparent in the cell cytosol. **G.** Micrograph depicting

two healthy Type I cells (green, left) and a dying Type II cell (purple, right). Arrows indicate mitochondria in healthy cells (left 2) and those of the dying cell (right 4). Scale bar is 1 µm and applies to **G, H, H', I,** and **I'**. **H.** Micrograph of healthy cell cytosol with arrows indicating Golgi bodies. **H'.** Enlarged region of cytosol including a healthy Golgi apparatus. **I.** Micrograph of a dying Type II cell with arrows indicating swollen Golgi bodies. **I'.** Enlarged region of the swollen Golgi apparatus of a dying cell.

Figure 3. Cell volumes of taste cells. Graph depicts total cell volumes of healthy Type II and III cells (left), early dying Type II and III cells (middle, light gray), and late stage dying cells (right, dark gray).

Figure 4. Lysosomes in taste cells. A. Reconstructions of selected taste cells (grey) and their lysosomes (color coded by size from small (blue) to large (red)). Reconstructions are divided into cell types: IV, III, II, I, early dying (**ed**), and late dying (**ld**). **B.** Lysosome count per cell (left) and lysosome median volume by cell (right). Each data point represents a single cell. Data is binned by cell type, as in **A. C.** Swarm charts of lysosome volumes of healthy Type II cells and early stage dying Type II cells showing the entire range of volumes (left) and a cropped view (right) of the volumes below 1µm^3. Black squares indicate mean volume, while diamonds indicate median volume. **D.** Reconstructions of the lysosome meshes from healthy Type II cells (blue) and an early stage dying Type II cells (purple). Inset shows an enlarged view of the perinuclear area from a healthy and dying cell.

685 **Figure 5. Morphological features of healthy and dying taste cell nuclei. A.**
686 Reconstruction of healthy Type II cell nucleus (blue) with distended regions between
687 inner and outer nuclear membranes reconstructed in gray. **B.** Micrograph of a healthy
688 Type II cell nucleus (that reconstructed in **A**) (blue, left) and a nucleus of a dying Type II
689 cell on the right (purple) showing distended regions between the inner and outer
690 nuclear membrane. Scale bar is 2 µm, and applies to all micrographs in this figure. **C.**
691 Reconstruction of the nucleus shown in **B**, showing in the inner nuclear region in purple,
692 and the distended regions between the inner nuclear membrane in lighter purple. Of
693 the dying cell nuclei, this is the only nucleus for which these distended regions were
694 segmented and reconstructed. Thus, the reconstructions in **E** and **G** do not feature
695 equivalent reconstructions of the distended nuclear membrane regions**. D, D'.**
696 Reconstruction (**D**) and micrograph (**D'**) of healthy Type II cell nucleus. **E, E'.**
697 Reconstruction (**E**) and micrograph (**E'**) of a fragmented nucleus of a dying cell of
698 unknown type. Arrows indicate regions of heterochromatin expansion. **F, F'.**
699 Reconstruction (**F**) and micrograph (**F'**) of a healthy Type III cell nucleus. **G, G'.**
700 Reconstruction (**G**) and micrograph (**G'**) of the shrunken nucleus of a dying cell of
701 unknown type. Arrows indicate regions of heterochromatin expansion.
702
703 **Figure 6. Synapses in dying cells. A.** Micrograph of the point of contact between a late
704 stage dying cell of unknown type (purple) and an adjacent nerve fiber (yellow). Asterisk
705 indicates region of contact. Scale bar is 1 µm and applies to all micrographs in this
706 figure. **B.** Synaptic sites between two nerve fibers (yellow-green and yellow) and a dying

Type II cell (purple). Arrows indicate atypical mitochondria (red), which feature abnormal cristae patterns. **C.** Reconstruction of a dying Type II cell (purple) and the three nerve fibers that receive synapses from it in the taste bud shell (gray). Atypical mitochondria are red. Only the orange fiber exits the base of the taste bud. The green and pink fibers appear to be nerve fiber fragments. Scale bar 10 µm. **D.** Micrograph showing a region of contact between a dying Type III cell (purple) and the adjacent nerve fiber (yellow). **E.** Enlarged micrograph showing a different point of contact between the dying Type III cell (purple) and the nerve fiber (yellow) in **D**. Arrows indicate large, swollen structures (upper arrow) and typical synaptic vesicle structures (lower arrow) at the point of contact with the nerve fiber. **F.** Reconstruction of a dying Type III cell (purple) and the nerve fiber it borders. This nerve fiber is a fragment and does not exit the base of the bud.

Figure 7. Type I cells as they relate to dying cells. A. Reconstruction of a late stage dying cell (purple) and the two Type I cells (green) that surround it. **B.** Micrograph of an early stage dying Type II cell (purple) and a neighboring Type I cell (green). Asterisk indicates a region of the dying cell nearly surrounded by the neighboring Type I cell, likely an area of phagocytosis. **C.** Micrograph of a late stage dying cell (purple) and the bordering Type I cell (green). Arrow indicates a presumed apoptotic body, which is completely surrounded by the Type I cell. **D.** Reconstruction of a late stage dying cell (purple) and the neighboring Type I cell (green). Lysosomes in the Type I cell are depicted in pink. **D'.** Rotated, enlarged view of the Type I cell partially surrounding the dying cell. **D''.**

729 Enlarged region of D which highlights the lysosomes (pink) in the region of the Type I cell
730 that borders the dying cell. **D'''.** Enlarged region of D which highlights the lysosomes
731 (pink) in the region of the Type I cell that does not border the dying cell. **E.** Micrograph
732 of a Type I cell (green) that borders an early dying cell (purple). Arrows indicate large,
733 membrane enclosed profiles that the Type I cell may have engulfed from the dying cell.
734 **E'.** Enlarged region of E which highlights the membrane continuity between the dying
735 cell and one such profile that is perhaps in the process of being engulfed by the
736 neighboring Type I cell.
737
738 **Figure 8. Dying cells in the context of the bud. A.** Pie charts depicting the cell type
739 composition of two taste buds: TF21 TB1 and TF21 TB2. These two taste buds are the
740 only taste buds that are fully contained in the boundaries of the tissue block. **B.** Diagram
741 depicting the locations of cell nuclei within the taste bud TF21 TB2 according to cell
742 type. Immature Type IV cell nuclei (pink-purple) are on the left, followed by Type III cell
743 nuclei (red), Type II cell nuclei (blue), Type I cell nuclei (green) and dying cell nuclei
744 (dusty purple). One nucleus in the Type II cell panel is labeled as purple (asterisk),
745 because the cell it inhabits is immature and we cannot discern whether it would have
746 developed into a Type II or Type III cell. The taste bud and nuclei are shown in profile
747 (top row) and from a top down view of the taste bud (bottom).
748
749 **Figure 9. Pathway to death.** Reconstructions of cells summarizing the pathway from
750 birth to death of a taste cell. From left to right: dividing basal cell, Type IV immature

taste cell, Immature Type II or III taste cell, Type II mature taste cell, Type II early stage dying cell, Late stage dying cell of unknown type.

Supplementary Figure 1. Estimation statistics for the median difference of cell volumes between cell categories. The median differences between healthy and late stage dying cells (**A**); early stage and late stage dying cells (**B**); healthy Type II and early stage dying Type II cells (**C**); and healthy Type III and early stage dying Type III cells (**D**) as shown in Gardner-Altman estimation plots generated using estimationstats.com (Ho et al., 2019). For each comparison, both groups are plotted on the left axes; the mean difference is plotted on a floating axes on the right as a bootstrap sampling distribution. The mean difference is depicted as a dot; the ends of the vertical error bar (black) indicate the 95% confidence interval. All calculated confidence intervals indicate that the compared groups are different.

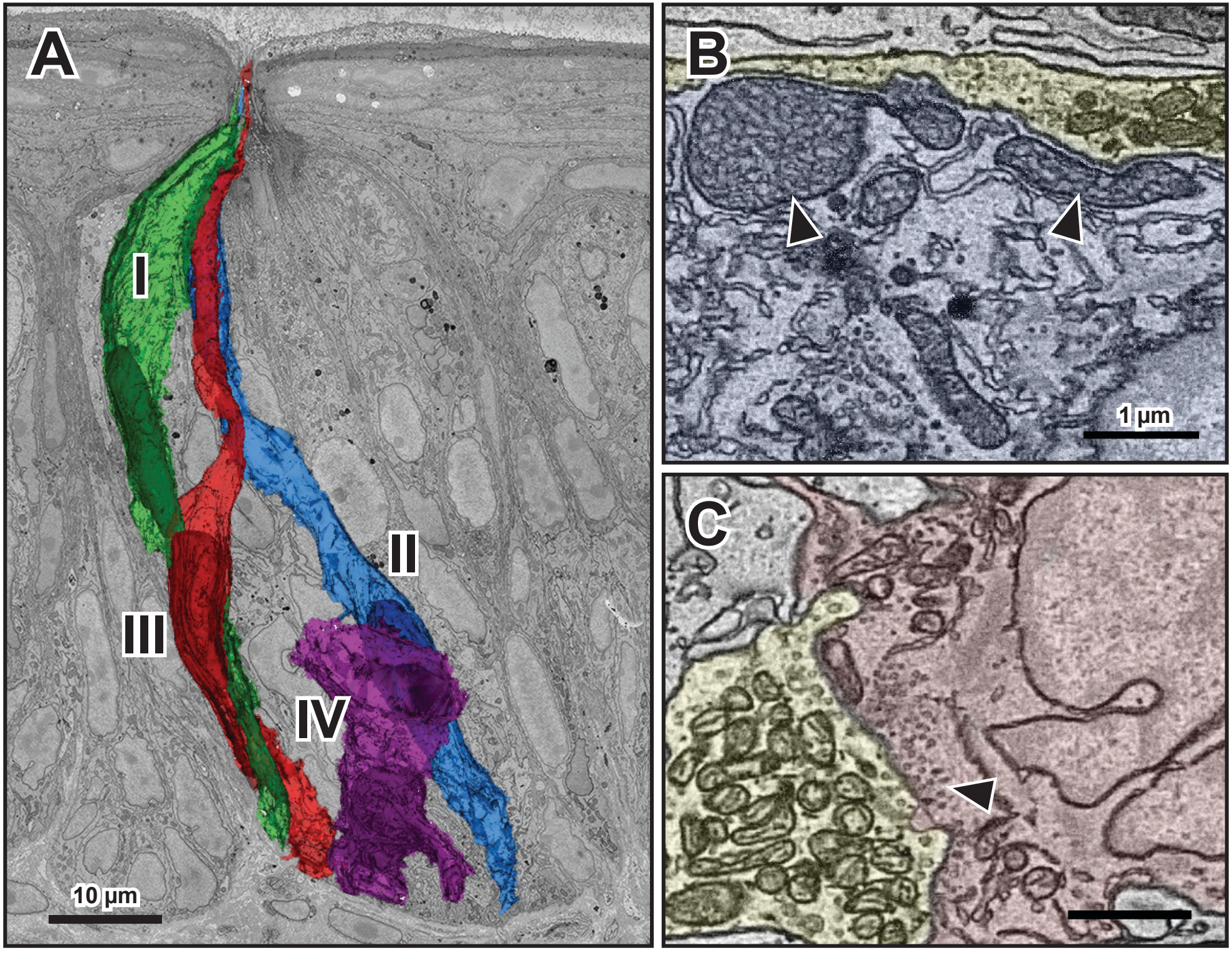
A
I
II
III
IV
10 µm
B
1 µm
C

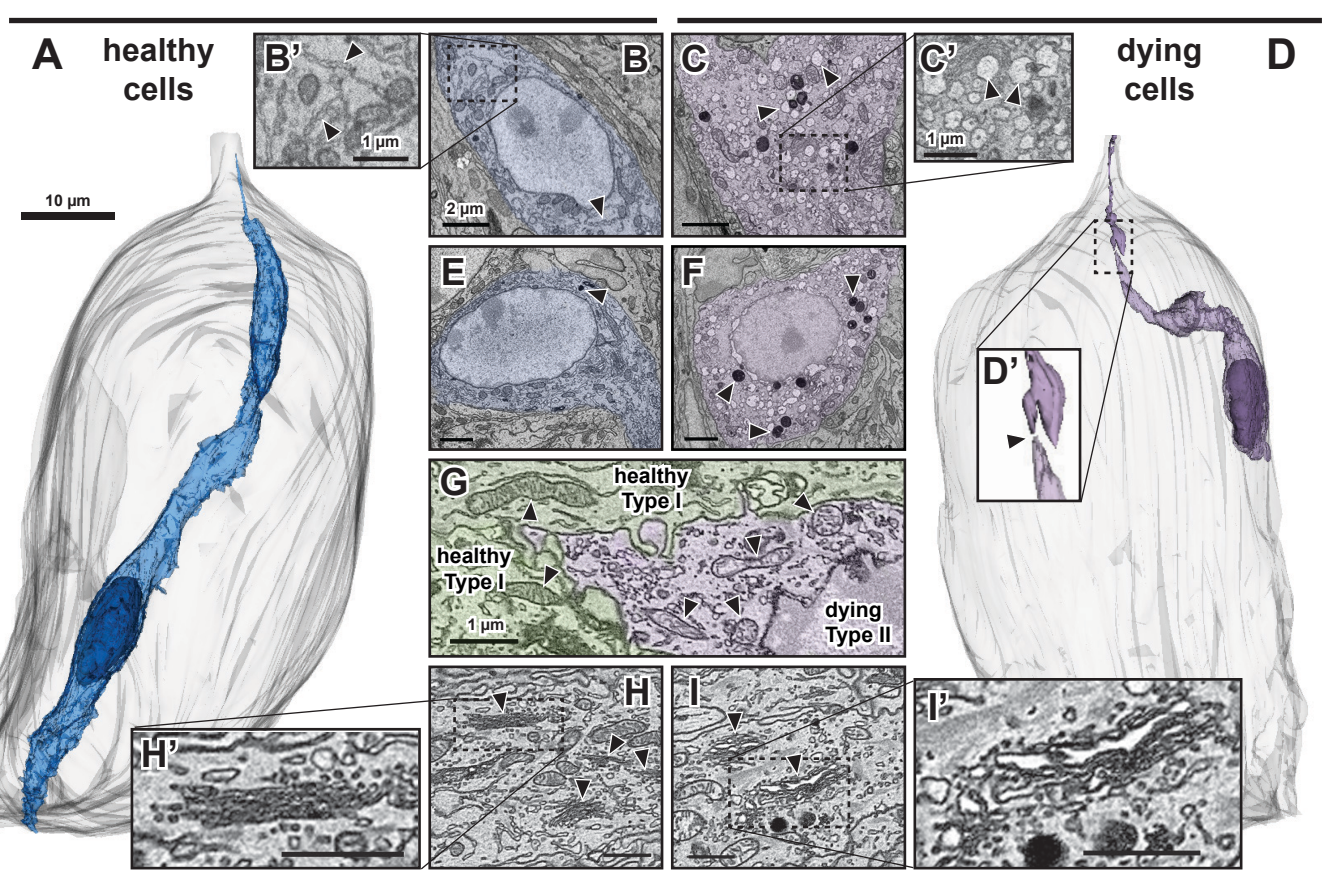
A
healthy cells
B'
1 µm
B
2 µm
C
C'
1 µm
dying cells
D
10 µm
E
F
D'
G
healthy Type I
healthy Type I
1 µm
dying Type II
H'
H
I
I'

cell volumes

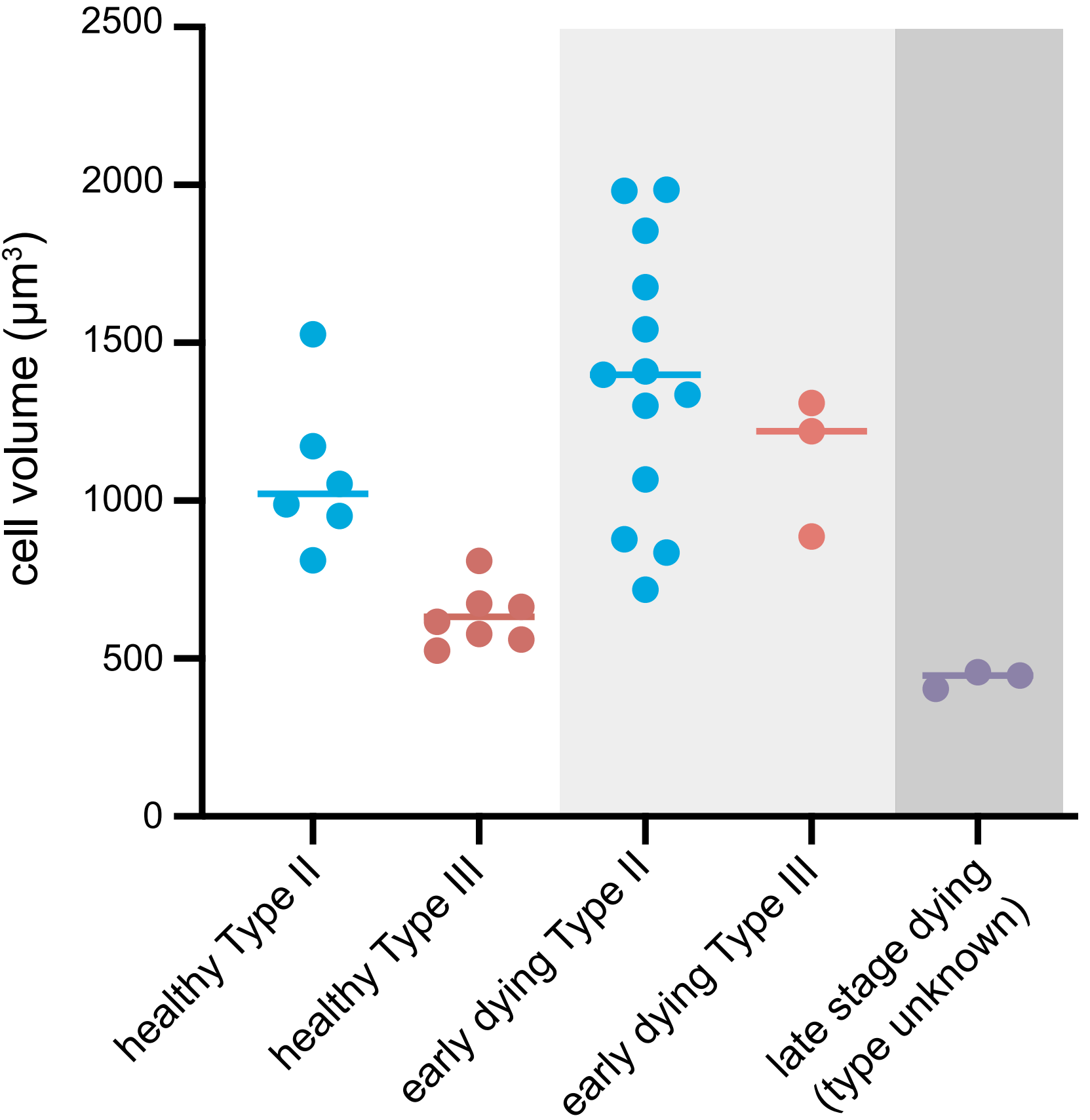

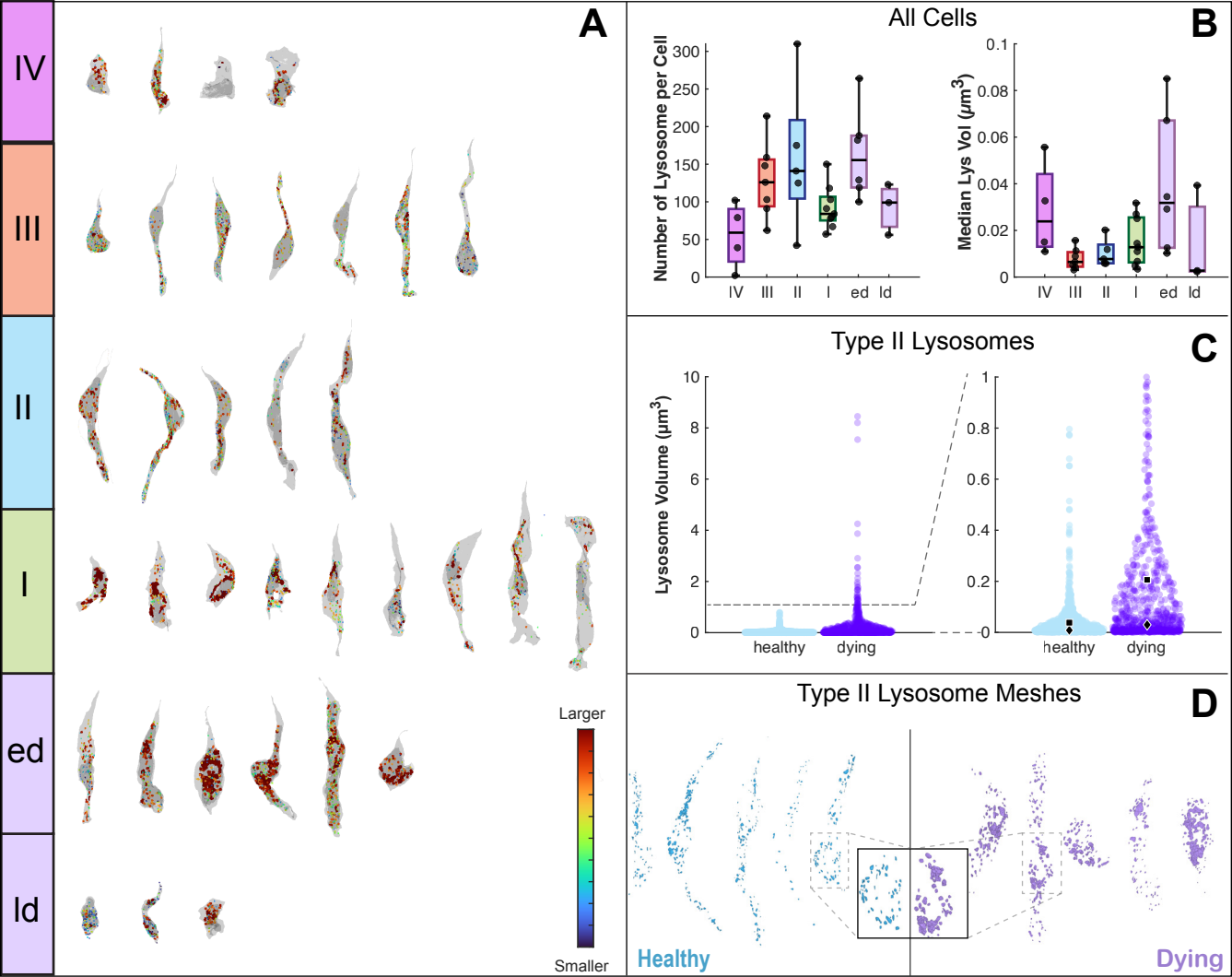
IV
III
II
I
ed
ld
A
Larger
Smaller
All Cells
B
Number of Lysosome per Cell
Median Lys Vol (μm3)
IV III II I ed ld
Type II Lysosomes
C
Lysosome Volume (μm3)
healthy
dying
Type II Lysosome Meshes
D
Healthy
Dying

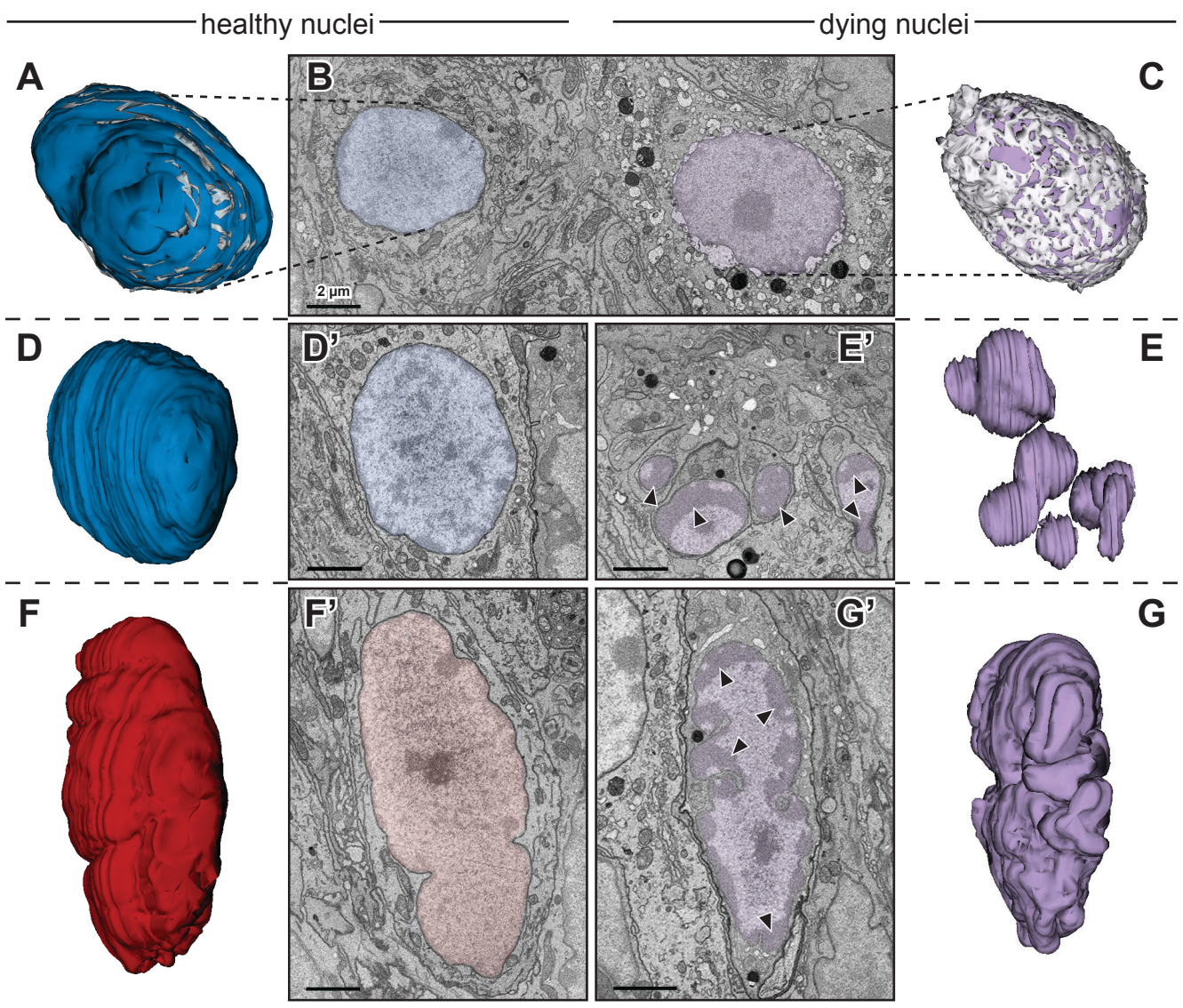
healthy nuclei
dying nuclei
A
B
C
2 µm
D
D'
E'
E
F
F'
G'
G

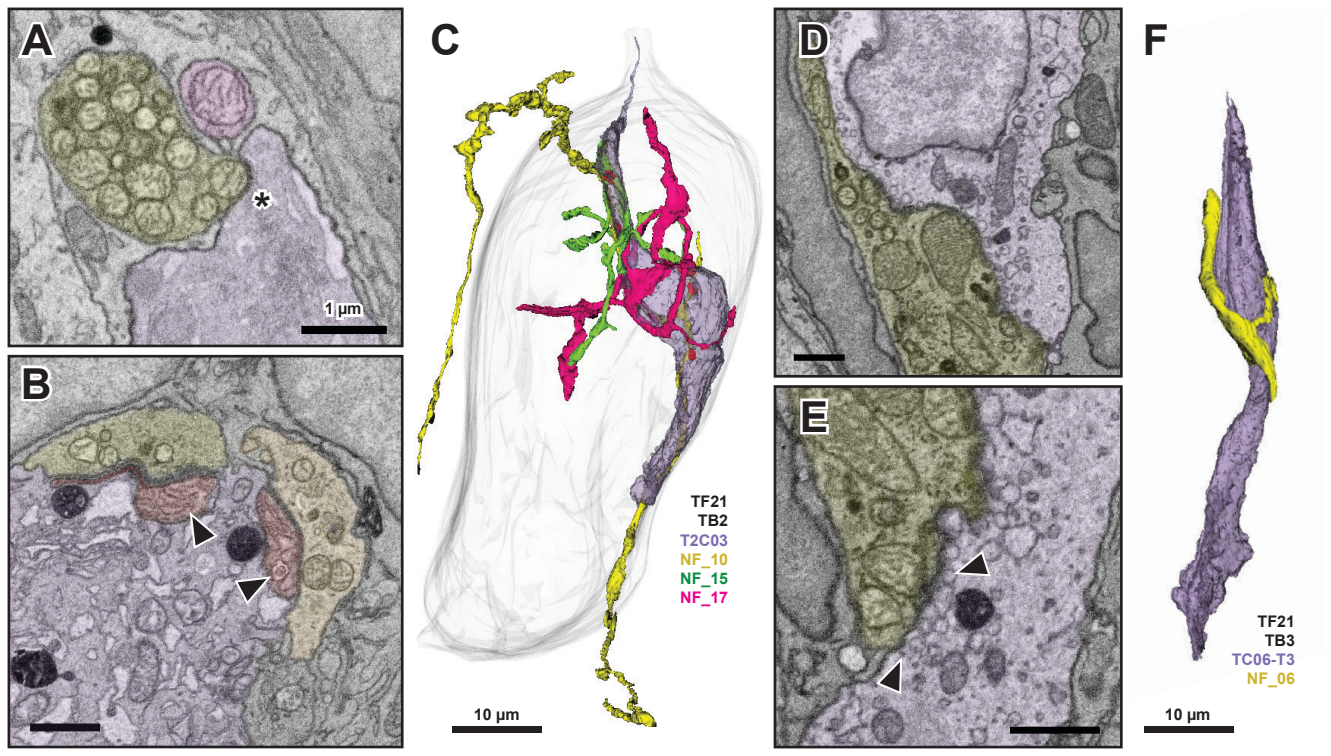
A
1 µm
B
C
TF21
TB2
T2C03
NF_10
NF_15
NF_17
10 µm
D
E
F
TF21
TB3
TC06-T3
NF_06
10 µm

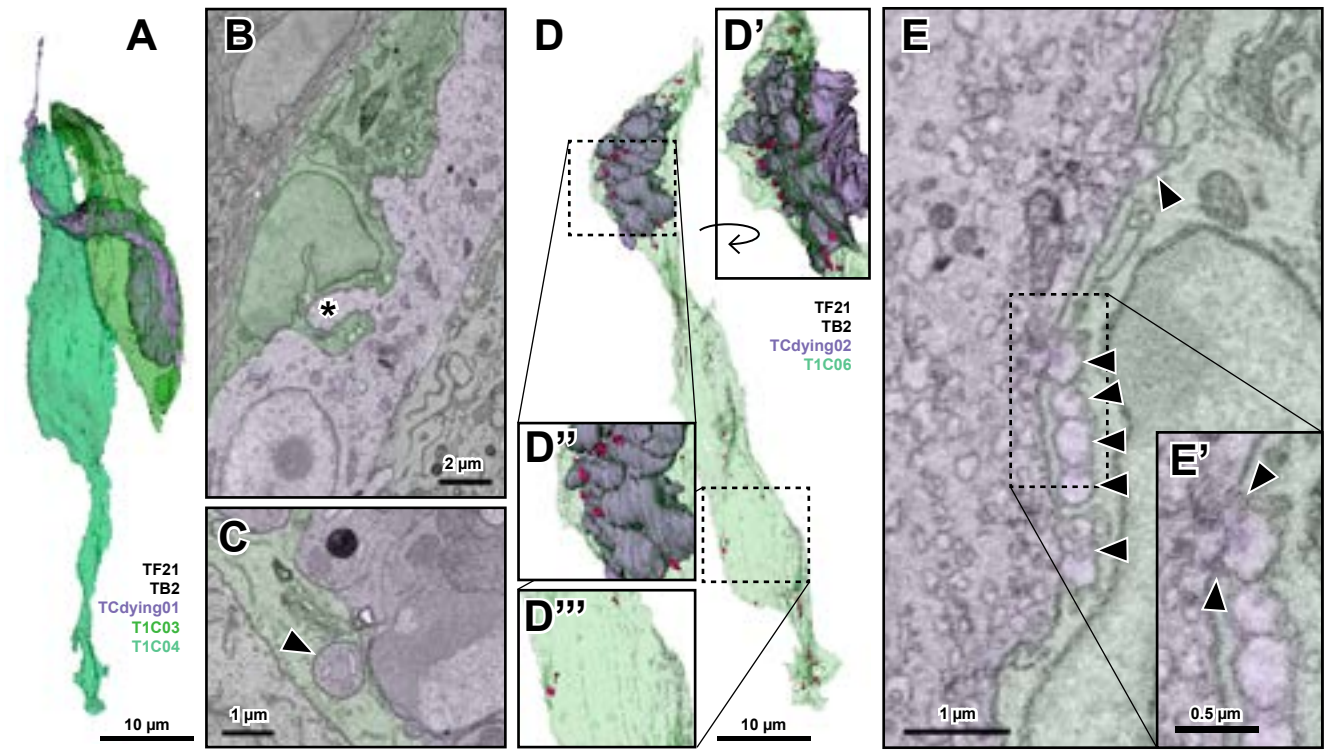
A
B
C
D
D'
D''
D'''
E
E'
TF21
TB2
TCdying01
T1C03
T1C04
TF21
TB2
TCdying02
T1C06
10 µm
2 µm
1 µm
10 µm
1 µm
0.5 µm

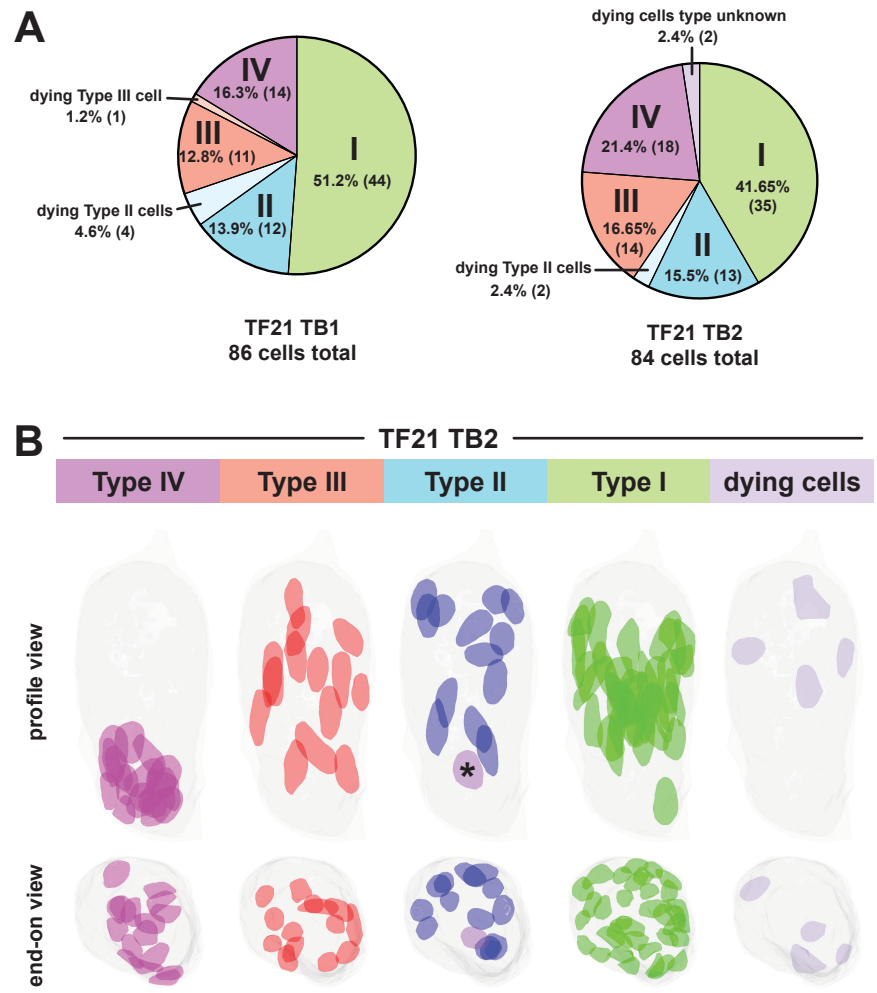
A
IV
16.3% (14)
dying Type III cell
1.2% (1)
III
12.8% (11)
I
51.2% (44)
dying Type II cells
4.6% (4)
II
13.9% (12)
TF21 TB1
86 cells total
dying cells type unknown
2.4% (2)
IV
21.4% (18)
I
41.65%
(35)
III
16.65%
(14)
dying Type II cells
2.4% (2)
II
15.5% (13)
TF21 TB2
84 cells total
B
TF21 TB2
Type IV
Type III
Type II
Type I
dying cells
profile view
end-on view
*

Pathway to Death

10 µm

DS2_basalcell05
basal

Dividing basal cell

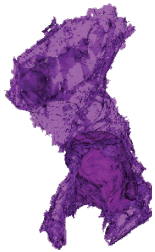

TF21_TB2_T4C-01
immature
cell type undetermined

Type IV immature taste cell

TF21_TB2_T3C19
immature
Type II or Type III

Immature elongate taste cell

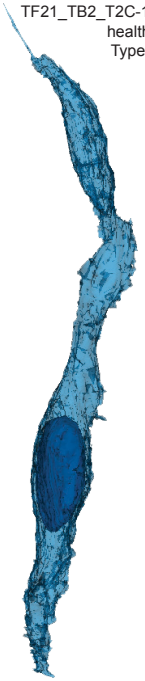

TF21_TB2_T2C-10
healthy
Type II

Mature taste cell

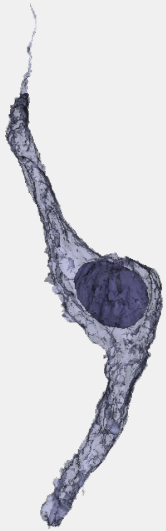

TF21_TB2_T2C-03
early stage dying
Type II

Early stage dying taste cell

TF21_TB2_TCdying02
late stage dying
cell type unknown

Late stage dying taste cell

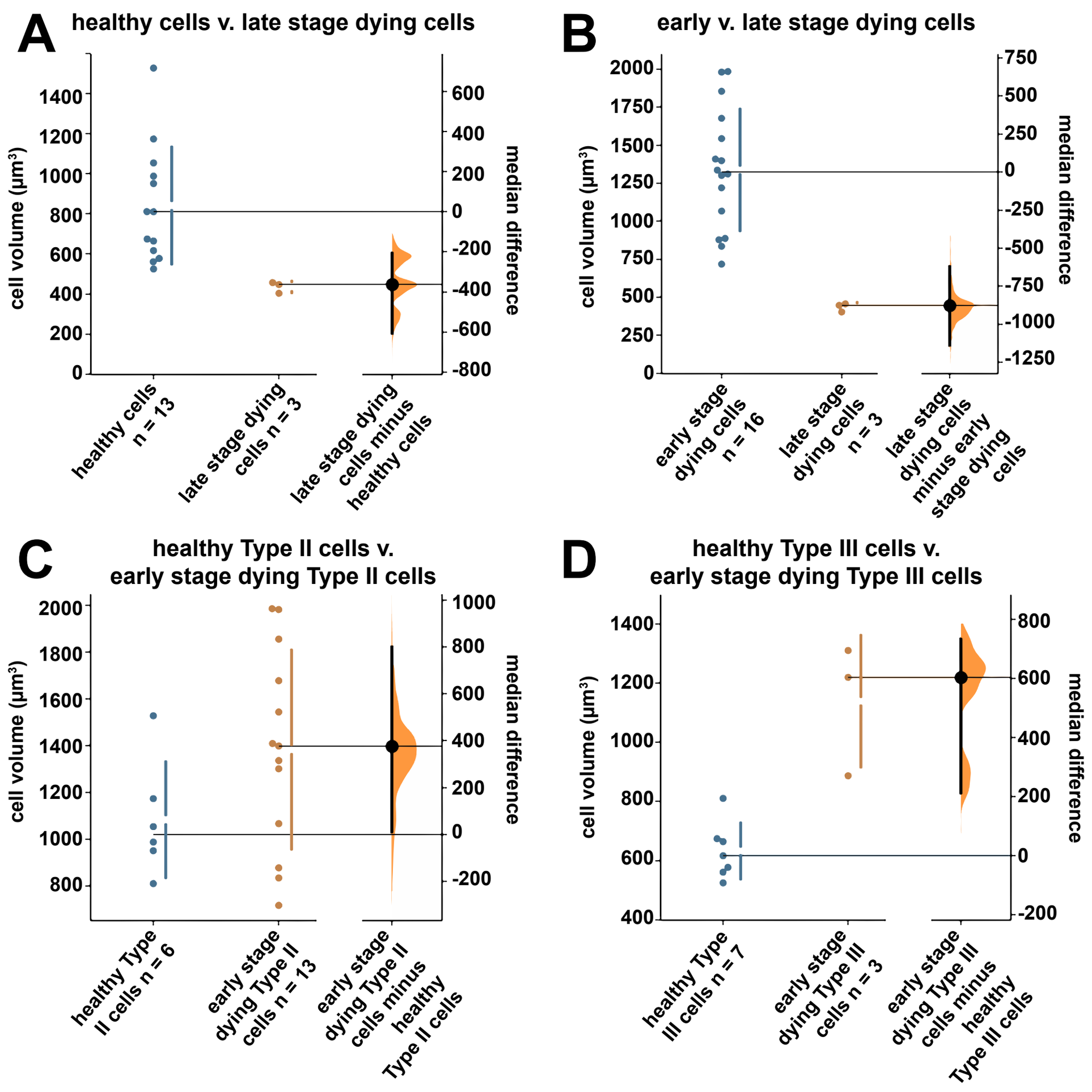
A
healthy cells v. late stage dying cells
cell volume (µm³)
median difference
healthy cells n = 13
late stage dying cells n = 3
late stage dying cells minus healthy cells
B
early v. late stage dying cells
cell volume (µm³)
median difference
early stage dying cells n = 16
late stage dying cells n = 3
late stage dying cells minus early stage dying cells
C
healthy Type II cells v. early stage dying Type II cells
cell volume (µm³)
median difference
healthy Type II cells n = 6
early stage dying Type II cells n = 13
early stage dying Type II cells minus healthy Type II cells
D
healthy Type III cells v. early stage dying Type III cells
cell volume (µm³)
median difference
healthy Type III cells n = 7
early stage dying Type III cells n = 3
early stage dying Type III cells minus healthy Type III cells